

# Phase states and thermomorphologic, thermotropic, and magnetomorphologic properties of lyotropic mesophases: Sodium lauryl sulphate–water–1-decanol liquid-crystalline system

Pınar Özden, Arif Nesrullajev,\* and Şener Oktik

*Faculty of Science and Letters, Department of Physics, Muğla University, 48000 Kötekli Muğla, Turkey*

(Received 3 February 2010; published 3 December 2010)

Phase states in sodium lauryl sulphate–water–1-decanol lyotropic liquid-crystalline system have been investigated for different temperature ranges. The dependence of triangle phase diagram types, phase boundaries, and sequence of lyotropic mesophases vs temperature has been found. The thermomorphologic, thermotropic, and magnetomorphologic properties of hexagonal E, lamellar D, nematic-calamitic  $N_C$ , nematic-discotic  $N_D$ , and biaxial nematic  $N_{bx}$  mesophases have been studied in detail. Dynamics of transformations of magnetically induced textures has been investigated. Peculiarities of typical and magnetically induced textures have been investigated in detail. Triangle phase diagrams of sodium lauryl sulphate–water–1-decanol lyotropic liquid-crystalline system for different temperatures and typical and magnetically induced textures of E, D,  $N_C$ ,  $N_D$ , and  $N_{bx}$  mesophases are presented.

DOI: [10.1103/PhysRevE.82.061701](https://doi.org/10.1103/PhysRevE.82.061701)

PACS number(s): 61.30.St, 61.30.Jf, 64.70.M–, 64.70.pp

## I. INTRODUCTION

Polymorphism and phase states of the ternary amphiphile-water-aliphatic alcohol lyotropic liquid-crystalline systems have been extensively studied over the past two-three decades. Extensive interest to lyotropic systems was because these systems are formed by the isometric and anisometric structural units, i.e., spherical, rodlike, and disklike micelles, and they exhibit various types of lyotropic phases and mesophases. In lyotropic systems, micelles arise due to the tendency of spontaneous creation of interfaces between polar and nonpolar groups of amphiphile molecules [1–5]. In these systems, lyotropic isotropic phases with the isometric micelles and lyotropic anisotropic mesophases with the anisometric micelles have definite phase sequences and are characterized by the phase diagrams.

The phase diagrams of lyotropic liquid crystals are usually very diverse and complex. Many different phases and mesophases arise in lyotropic systems as the function of concentration and temperature with typical textures, specific structures, and definite spatial symmetry [6–9]. A variety of structural properties, types of the physical anisotropy, and differences in spatial symmetry lead to differences in the physical properties of lyotropic phases and mesophases. Therefore, studies on the phase states in lyotropic systems and also comparative investigations of the connection between the microscopic and macroscopic properties of lyotropic mesophases are important topics in the physics and physical chemistry of lyotropic systems. On the other hand, mesophases of lyotropic systems have different types of the optical, diamagnetic, dielectric, viscous elastic, etc., anisotropies and are very sensitive to various external effects and boundary conditions [10–13]. These effects and boundary conditions lead to changes of the physical peculiarities and to the appearance of stimulated properties in lyotropic mesophases. Therefore, investigations of the external effects on the physical properties of lyotropic mesophases are im-

portant topics from both fundamental and application points of view.

In this work, we are interested in the temperature dependence of the phase states and in the character of the phase diagrams of the ternary sodium lauryl sulphate (sodium dodecylsulphate) (SLS)–water ( $H_2O$ )–1-decanol (DeOH) lyotropic system for different temperatures. We are also interested in detailed investigations on the orientational, thermomorphologic, thermotropic, and magnetomorphologic properties of hexagonal E, lamellar D, nematic-calamitic  $N_C$ , nematic-discotic  $N_D$ , and biaxial nematic  $N_{bx}$  mesophases taking place in this lyotropic system. Results of these investigations are presented in this work.

## II. MATERIALS AND TECHNIQUES

SLS was purchased from Merck and was purified by recrystallization from ether or ethanol. DeOH was also purchased from Merck, had a high degree of purity, and was used without further purification. Water, which was used as general solvent, was triple distilled and de-ionized. The preparation process of lyotropic liquid-crystalline systems followed known procedures. SLS and water were weighed into glass ampoules with an accuracy of  $\pm 10^{-4}$  g. After homogenization for some days at 313 K in a thermostat, 1-decanol was added in this mixture. Such lyotropic mixture in hermetically closed ampoule was periodically mixed by a shaker and kept in a thermostat at 313 K for one week. Homogeneity of the obtained lyotropic mixture was examined by crossed polarizers and by studies of textures using a polarizing optical microscope.

Microslide samples such as sandwich cells were used in this study. The thickness of the liquid-crystalline layer in the microslides was 120  $\mu\text{m}$ . The microslides were hermetically closed at once after filling by liquid-crystalline system.

A permanent magnet was used for the experiments carried out to obtain magnetically induced and aligned textures of lyotropic mesophases. The magnetic field was applied orthogonally to the reference surfaces of the microslides and accordingly to a liquid-crystalline layer. Fields of 9.7 kG

\*Corresponding author; arifnesr@mu.edu.tr

were available. During the magnetic field influence, the samples were kept at a stable temperature of 297.0 K.

The polarizing optical microscopy method was used for thermomorphologic investigations. Our setup consisted of a trinocular polarizing microscope with orthoscopic and/or conoscopic observations, a microphotographic system, and a Berek compensator from Olympus Optical Co.,  $\lambda$  plates ( $\lambda = 137 \mu\text{m}$  and  $\lambda = 530 \mu\text{m}$ ), a heater-thermostat with digital temperature control system, differential Cu-Co thermocouples, power supply, and multimeters. The thermotropic and thermomorphologic properties of the biphasic regions of the direct *mesophase-isotropic liquid* and the reverse *isotropic liquid-mesophase* phase transitions have been studied using the capillary temperature wedge (CTW) device. This device is presented in [14,15]. The CTW allows us to obtain simultaneously all thermal states of liquid-crystalline material, to study the thermotropic properties of these states, and to calculate the linear and temperature widths of the biphasic regions of the thermotropic phase transitions with an accuracy of not less than  $\pm 2.0 \times 10^{-3} \text{ mm}$  and  $\pm 10^{-3} \text{ K}$  accordingly [15,16]. The optical mapping (OM) method was employed to investigate the peculiarities of typical textures and magnetically induced textures in lyotropic liquid-crystalline mesophases and to determine the optical signs and the disclinations of strength for various singularities that take place in the textures of these mesophases. The OM method is presented in [17,18] and was widely used in [19–22] for detailed investigations of the peculiarities of liquid-crystalline textures.

### III. RESULTS AND DISCUSSIONS

#### A. Mesomorphism and morphology of SLS-H<sub>2</sub>O-DeOH lyotropic system

In this work, the phase states and the mesomorphic and morphologic properties of SLS-H<sub>2</sub>O-DeOH lyotropic liquid-crystalline system have been studied. Our objectives were as follows. The phase diagrams of SLS-H<sub>2</sub>O-DeOH lyotropic system are presented in a number of works [1,23–34]. However, the number and types of mesophases on these phase diagrams are different. Additionally, the concentration regions of the interface boundaries of lyotropic phases and mesophases on these diagrams are also different. Namely, for SLS-H<sub>2</sub>O-DeOH lyotropic system, (a) isotropic micellar L<sub>1</sub> phase and hexagonal E and lamellar D mesophases in [1,26], (b) L<sub>1</sub> phase and E, D, and nematic-calamitic N<sub>C</sub> mesophases in [27], (c) L<sub>1</sub> phase and E, D, N<sub>C</sub>, and nematic-discotic N<sub>D</sub> mesophases in [28,30,31,33,34], (d) L<sub>1</sub> phase and E, D, N<sub>C</sub>, N<sub>D</sub>, and biaxial nematic N<sub>bx</sub> mesophases in [32] have been found. Besides, by zero decanol concentration for SLS-water lyotropic system, (a) L<sub>1</sub> and cubic phases and E and D mesophases in [23], (b) L<sub>1</sub> phase and E, complex hexagonal H<sub>C</sub>, and D mesophases in [25], and (c) L<sub>1</sub> phase and E and D mesophases in [26,29] have been found.

Because of such variety of the mesomorphic properties and the phase states in SLS-H<sub>2</sub>O-DeOH lyotropic system we carried out preliminary investigations on the mesomorphic and morphologic properties and the phase states of this system. The investigations showed that the number of lyotropic

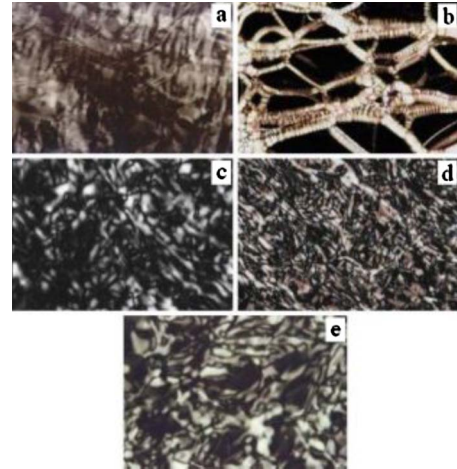


FIG. 1. (Color online) Main textures of mesophases in SLS-H<sub>2</sub>O-DeOH lyotropic system. Crossed polarizers. Magnification of  $\times 100$ . Temperature of 297.0 K. (a) Hexagonal E mesophase, (b) lamellar D mesophase, (c) nematic-calamitic N<sub>C</sub> mesophase, (d) nematic-discotic N<sub>D</sub> mesophase, and (e) biaxial nematic N<sub>bx</sub> mesophase.

liquid-crystalline mesophases and concentration boundaries between these mesophases on the phase diagram of SLS-H<sub>2</sub>O-DeOH lyotropic system depend on temperature. The investigations showed also that five main types of liquid-crystalline textures are observed in this system (Fig. 1). These textures correspond to E, D, N<sub>C</sub>, N<sub>D</sub>, and N<sub>bx</sub> mesophases.

E mesophase is a uniaxial optically negative mesophase, which is formed by the rodlike micelles of quasi-infinite lengths in hexagonal packing. This mesophase displays a fibrous texture [Fig. 1(a)]. This texture is specific for E mesophase, has low birefringence, and consists of the prolonged filamentlike formations and uniform regions with planar and titled orientation. Such type of texture for E mesophase has been observed in various lyotropic systems [1,35–37].

D mesophase is a uniaxial optically positive mesophase, which is formed by the platelike micelles (lamellas) of quasi-infinite diameter in layered packing. This mesophase displays a texture with the oily streaks under pseudoisotropic anchoring conditions [Fig. 1(b)]. The oily streaks are the birefringent bands which consist of small confocal formations. These bands form the net on the homeotropic background. Such type of texture for D mesophase is specific and has been observed in various lyotropic systems [5,37–41]. We would like to note that textures with the oily streaks have been also observed in thermotropic cholesteric mesophase [41–46]. However, in thermotropic cholesteric mesophase, the oily streaks arise on the planar and optical active background but not on the pseudoisotropic background as in D mesophase.

N<sub>C</sub> and N<sub>D</sub> mesophases are optically uniaxial. These mesophases display the typical schlieren textures [Figs. 1(c) and 1(d)]. Textures of N<sub>C</sub> and N<sub>D</sub> mesophases consist of several threadlike formations, singular points, and small uniform regions. In the uniform regions of N<sub>C</sub> mesophase, the rodlike micelles are oriented parallel to the reference surfaces of the microslides. In this case, the director is oriented parallel to

the reference surfaces of the microslides and amphiphile molecules in the rodlike micelles are oriented perpendicular to these surfaces. In the uniform regions of  $N_D$  mesophase, the bilayer disklike micelles are oriented parallel to the reference surfaces of the microslides. In this case, the director and amphiphile molecules in the disklike micelles are oriented perpendicular to the reference surfaces of the microslides. The arrangement of the optical axis and amphiphile molecules is caused by the negative optical birefringence ( $\Delta n = n_{\parallel} - n_{\perp} < 0$ ) for  $N_C$  mesophase and the positive optical birefringence ( $\Delta n = n_{\parallel} - n_{\perp} > 0$ ) for  $N_D$  mesophase. Such type of textures for lyotropic nematic mesophases has been observed in various lyotropic systems for  $N_C$  mesophase in [37,47–50] and for  $N_D$  mesophase in [37,47,50–52].

$N_{bx}$  mesophase is optically biaxial. This mesophase is characterized by the tensor of second rank and two macroscopic order parameters [53,54].  $N_{bx}$  mesophase displays the specific texture, which is presented in Fig. 1(e). This texture is the smooth schlieren texture and consists of the looplike formations and uniform regions with the homeotropic and planar alignment. The birefringence of the planar aligned regions has been determined as  $\Delta n = 0.0044$ . These uniform regions are characterized by different directions of the diamagnetic susceptibility axis. For uniform regions with minimal magnetic susceptibility, the axis is parallel to the reference surfaces of the microslide, while for the uniform regions with maximal magnetic susceptibility the axis is perpendicular to the surfaces. This texture was observed in small temperature and concentration intervals. Such type of texture for  $N_{bx}$  mesophase has been observed in various lyotropic systems [50,51].  $N_{bx}$  mesophase is an intermediate mesophase between two uniaxial  $N_C$  and  $N_D$  mesophases. The conoscopic observations and investigations of the thermo-optical properties were utilized to establish the existence of  $N_{bx}$  mesophase between  $N_C$  and  $N_D$  mesophases for sodium dodecylsulphate–water–1-decanol, sodium dodecylsulphate–water–1-decanol, and potassium laurate (KL)–water–1-decanol lyotropic systems [32,55–58].

Textures of E, D,  $N_C$ ,  $N_D$ , and  $N_{bx}$  mesophases have been observed in strongly definite concentration and temperature intervals and were stable and repeatable.

### B. Phase states of SLS-H<sub>2</sub>O-DeOH lyotropic system

Investigations showed that the character of the triangle phase diagram of SLS-H<sub>2</sub>O-DeOH lyotropic system depends on temperature. Figure 2(a) presents the triangle phase diagram of this system at 297.5 K. As seen in this figure, at 297.5 K  $L_1$  phase and E, D,  $N_C$ ,  $N_{bx}$ , and  $N_D$  mesophases take place. These mesophases were observed in strongly definite concentration intervals. Between  $L_1$  phase and E, D,  $N_C$ ,  $N_{bx}$ , and  $N_D$  mesophases the lyotropic transition regions take place. The number of lyotropic mesophases and their sequence in diagram, presented in Fig. 2(a), are in good agreement with the number and sequence of the mesophases presented in [32]. Differences in concentration intervals of lyotropic mesophases can be connected with differences in the purity of SLS and in the temperatures for the diagrams,

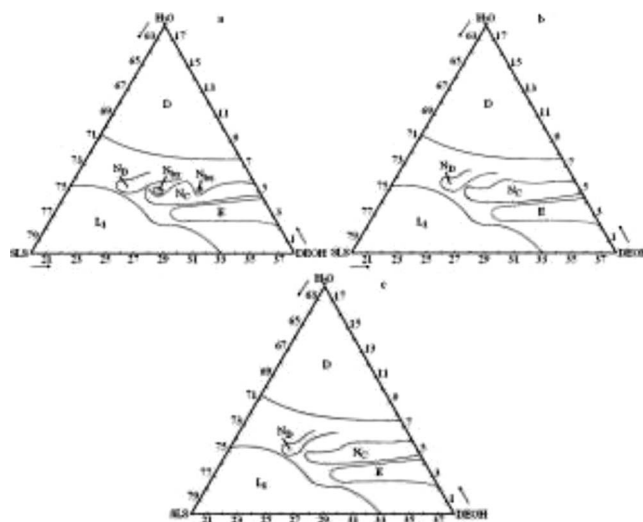


FIG. 2. Phase diagrams of SLS-H<sub>2</sub>O-DeOH lyotropic system. (a) 297.5 K, (b) 303.0 K, and (c) 311.0 K.

presented in this work and in [32]. Besides, in our work, the triple distilled and de-ionized water was used as the general solvent, whereas D<sub>2</sub>O from Sigma was used in [32].

We found that a change in the temperature leads to a change in the concentration intervals of the mesophases in SLS-H<sub>2</sub>O-DeOH system and to a change in the number of mesophases. In Figs. 2(b) and 2(c), the triangle phase diagrams of this system at 303 and 311 K are presented. As it is seen by comparison of the phase diagrams presented in Figs. 2(a)–2(c), an increase in temperature leads to a change of character of the triangle phase diagrams. Namely, by an increase of temperature of SLS-H<sub>2</sub>O-DeOH lyotropic system, an increase of the transition regions between  $N_C$ ,  $N_{bx}$ , and  $N_D$  mesophases, decrease of concentration intervals of these mesophases, and disappearance of  $N_{bx}$  mesophase take place. This result is obviously connected with the temperature sensitivities of these mesophases, which are formed by micelles with definite sizes, and also with the temperature dependences of lyotropic phase transitions. By change of temperature, the thermotropic phase transitions and transformations between lyotropic liquid-crystalline mesophases take place. Such transformations lead to change of intervals of these mesophases and their heterophase regions.

Disappearance of  $N_{bx}$  mesophase by an increase of temperature is connected with the fact that in lyotropic liquid-crystalline systems, this mesophase takes place not only in the narrow concentration region but also in the narrow temperature interval. We found that  $N_{bx}$  mesophase takes place in temperature interval as 3.6 K. This mesophase has been found in sufficiently narrow concentration and temperature intervals also in sodium decylsulphate (SDS)-H<sub>2</sub>O-DeOH, SDS-H<sub>2</sub>O-DeOH-sodium sulphate, KL-H<sub>2</sub>O-DeOH, KL-D<sub>2</sub>O-DeOH, and KL-DeOH-decylammonium chloride lyotropic systems by various scientists [59–64]. On the other hand, the change of concentration boundaries of E and D mesophases by temperature increase has not been observed for SLS-H<sub>2</sub>O-DeOH lyotropic system. This fact indicates a low sensitivity and the thermal and concentration stability of mesophases, which are formed by micelles with quasi-infinite sizes.

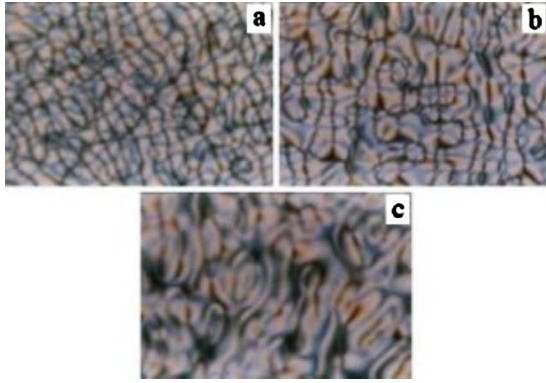


FIG. 3. (Color online) Magnetically induced textures of E mesophase. Crossed polarizers. Magnification of  $\times 100$ . Temperature of 297.0 K. (a) After 1.5 h, (b) after 3.5 h, and (c) after 6.0 h.

### C. Magnetomorphologic properties of E, D, $N_C$ , and $N_D$ mesophases

In this work, the magnetomorphologic properties of E, D,  $N_C$ ,  $N_{bx}$ , and  $N_D$  mesophases of SLS- $H_2O$ -DeOH lyotropic liquid-crystalline system have been investigated. The investigations showed that magnetic field has an influence on the morphologic and orientational properties of these mesophases and is efficient for obtain of the nonequilibrium magnetically induced textures. Additionally, when compared to E and D mesophases, intensive texture transformations within temperature and concentration intervals have been observed for  $N_C$ ,  $N_{bx}$ , and  $N_D$  mesophases.

*E mesophase.* The research revealed that under the effect of the magnetic field, changes of texture types take place. Besides, most changes of textures were observed during first 5–6 h. Figure 3 presents the magnetically induced textures of E mesophase, which were observed for different times. As seen in this figure, under the influence of magnetic field transformations of the fibrous texture [Fig. 1(a)] to textures with the loops take place. These loops are the peculiar inversion walls and represent the boundaries between little separate regions with uniform alignment. The sizes of these regions were determined as 7–12  $\mu\text{m}$ . The inversion walls in the case of E mesophase are not so sharp as in the case of lyotropic nematic mesophases [13,50,65,66]. In the course of time, under influence of the external magnetic field, change of shapes and displacement of the inversion walls has been observed (Fig. 3). Unlike the textures of lyotropic nematic mesophases, singular points have not been observed in magnetically induced textures of E mesophase. This fact indicates that the linear singularities, which are perpendicular to the liquid-crystalline layer, do not emerge in E mesophase. We would like to note that the type of texture, presented in Fig. 3(c), did not change for 48 h under influence of the magnetic field.

*D mesophase.* The investigations showed that magnetic field does not have sufficient influence on the morphologic properties of D mesophase. For a long time, only a weak change of density and displacement of the oily streaks and also small changes of the pseudoisotropic regions were observed in this mesophase (Fig. 4). This fact is connected with

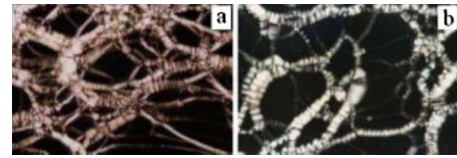


FIG. 4. (Color online) Magnetically induced textures of D mesophase. Crossed polarizers. Magnification of  $\times 100$ . Temperature of 297.0 K. (a) After 15–20 min and (b) after 3.5 h.

high viscosity of D mesophase and low mobility of lamellas. After 24 h, the regions between the oily streaks were characterized by the inexplicit conoscopic cross.

*$N_C$  mesophase.* The schlieren texture, which is characteristic for this mesophase, is stable and reproducible [Fig. 1(c)]. This texture was displayed again after the heating-cooling processes. We would like to note that  $N_C$  mesophase exhibits more stable thermomorphologic properties than  $N_D$  and  $N_{bx}$  mesophases.

The investigations showed that the process of texture transformations in  $N_C$  mesophase under the effect of magnetic field is complicated. Certain stages and types of magnetically induced textures were observed for this mesophase. The application of magnetic field after 1.5 h, the optical picture, as presented in Fig. 5(a), was observed. As is clear from the figure, the texture consists of a dense net of the loops and a number of the singular points. The loops are the boundaries between the separate uniformly oriented regions and characterize the break of the optical continuity in texture. Optical investigations showed that the singular points are the wedge disclinations which are placed orthogonally to the reference surfaces of the microslides. Experiments carried out using the optical mapping technique allow determining the optical signs of the singularities. Here, singularities with both positive and negative optical signs took place, but only with the disclination of the strength as  $|S|=1$ .

The density of the free energy of liquid crystal near the disclination lines in the spherical volume with radius  $R$  for single constant approximation can be determined by

$$\Phi = \Phi_1 + \Phi_2 + \Phi_{12}. \quad (1)$$

Here,  $\Phi_1$  and  $\Phi_2$  are the energies of separate disclinations per unit length between singularities and  $\Phi_{12}$  is the energy of

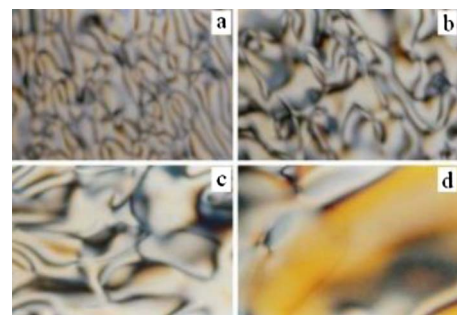


FIG. 5. (Color online) Magnetically induced textures of  $N_C$  mesophase. Crossed polarizers. Magnification of  $\times 100$ . Temperature of 297.0 K. (a) After 1.5 h, (b) after 3.5 h, (c) after 6.5 h, and (d) after 24.0 h.

interaction between these disclinations.  $\Phi_{12}$  is determined by [67–69]

$$\Phi_{12} = 2\pi K S_1 S_2 \ln \frac{2R}{r}. \quad (2)$$

Here,  $K$  is the elastic constant for the single constant approximation ( $K=K_{11}=K_{22}=K_{33}$ ),  $S_1$  and  $S_2$  are the disclinations of strength for connected singularities, and  $r$  is the distance between singularities. In accordance with the theoretical approach, as presented in [67–69], the interaction force between singularities can be determined by

$$F_{12} = \frac{\partial \Phi_{12}}{\partial r} = \frac{2\pi K S_1 S_2}{r}. \quad (3)$$

If the disclinations have the same sign, i.e., in the case of  $S_1 S_2 > 0$ , they push each other; if the disclinations have the opposite signs, i.e., in the case of  $S_1 S_2 < 0$ , they attract each other. In the case of singularities with the same disclination of strength, i.e., in the case of  $S_1 = S_2 = S$  the interaction force can be determined by

$$F_{12} = \frac{2\pi K S^2}{r}. \quad (4)$$

By taking into consideration the elastic constant of lyotropic nematic mesophase as  $K \sim 10^{-12}$  N [64,65,70] and distance between singularities presented in Fig. 5(a) as  $\sim 8-20$   $\mu\text{m}$ , the mean interaction force was determined as  $F_{12} = 0.8 \times 10^{-6} - 0.3 \times 10^{-6}$  N  $\text{m}^{-1}$ .

After 3.5 h, it was observed that the density of the loops decreased, while the sizes of uniformly oriented regions increased [Fig. 5(b)]. Optical investigations showed that inversion walls of the first and second orders also take place in this texture. After 6.5 h texture presented in Fig. 5(c) has been observed. In this texture, the sizes of uniformly oriented regions increased in comparison to the cases presented in Figs. 5(a) and 5(b). The inversion walls in this texture are the lines that unite the wedge disclinations. Unremitting texture transformations under magnetic field continued and after 24 h, the texture, presented in Fig. 5(c), was observed. In this texture, large layered planar regions and separate defects were observed. The birefringence of these regions was determined as  $\Delta n = 0.0043$ . Later, sufficient texture transformations in  $N_C$  mesophase were not observed.

$N_D$  mesophase. The schlieren texture [Fig. 1(d)], which is characteristic for this mesophase, was not stable. In time this texture transformed to the planar texture with the inversion walls [Fig. 6(a)]. The birefringence of these regions was  $\Delta n = 0.0045$ . The inversion walls, which are dependent on crossed polarizers position, are nearly parallel dark or light lines. The walls were placed perpendicularly to the liquid-crystalline layer and were transitional regions between the planar oriented regions. We would like to note that instability of the schlieren textures in  $N_D$  mesophase was observed also in [71].

As the investigations revealed, certain stages and types of magnetically oriented textures take place for  $N_D$  mesophase as well. At times, the domain texture arises during the process of the magnetomorphologic transformations in  $N_D$  me-

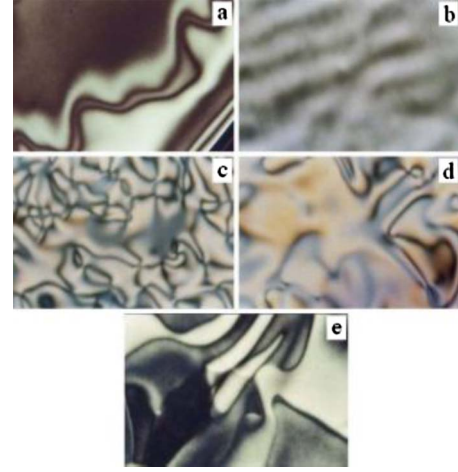


FIG. 6. (Color online) (a) Stable texture and (b)–(g) magnetically induced textures of  $N_D$  mesophase. Crossed polarizers. Magnification of  $\times 100$ . Temperature of 297.0 K. (a) Without field, (b) domain texture, (c) after 2.5 h, (d) after 6.5 h, and (e) after 24.0 h.

sophase [Fig. 6(b)]. Such type of the domain texture has also been observed by various scientists for  $N_C$  mesophase with both positive ( $\Delta\chi > 0$ ) and negative ( $\Delta\chi < 0$ ) diamagnetic anisotropies and for  $N_D$  mesophase with  $\Delta\chi < 0$  [6,13,65,66]. Such type of texture arises in  $N_D$  mesophase sufficiently rarely. Appearance of such type of the domain texture is connected with the effect of reverse flow. As a result of the flow, which takes place perpendicular to the domains, the cylindrical lenses arise [65,72]. We would like to note that the velocity of reverse flow in the case of  $N_C$  mesophase is bigger than in the case of  $N_D$  mesophase. This fact is attributed to the differences between the Leslie coefficients for  $N_C$  and  $N_D$  mesophases [6,68,73]. The flow alignment angle  $\theta$  is determined as

$$\cos 2\theta = -\frac{\gamma_1}{\gamma_2}, \quad (5)$$

where  $\gamma_1$  and  $\gamma_2$  are the Leslie coefficients [6]. For  $N_C$  mesophase,  $\theta \rightarrow 0$  and  $\gamma_1 \geq -\gamma_2$  and for  $N_D$  mesophase,  $\theta \rightarrow \pi/2$  and  $\gamma_1 \leq \gamma_2$  take place. The magnitude of the hydrodynamic term, which can lead to a back flow, is determined for the homeotropic  $\rightarrow$  planar transition by [74]

$$\lambda = \frac{\gamma_2 - \gamma_1}{2\gamma_1} \quad (6)$$

and for the planar  $\rightarrow$  homeotropic transition by [73]

$$\lambda_1 = \frac{\gamma_2 + \gamma_1}{2\gamma_1}. \quad (7)$$

Thus, Eq. (6) predicts strong back flow for the homeotropic  $\rightarrow$  planar transition in  $N_C$  mesophase with the rodlike micelles and Eq. (7) predicts weak back flow for the planar  $\rightarrow$  homeotropic transition in  $N_D$  mesophase. Therefore, the above-mentioned domains arise easier in  $N_C$  mesophase than in  $N_D$  mesophase.

After 2.5 h, the texture presented in Fig. 6(c) was observed. This texture consists of a lot of singular points and

loop formations. These loop formations are the tilted inversion walls. Optical investigations showed that the singularities with both positive and negative optical signs take place in this texture. In the case of singularities with positive optical signs, the brushes rotate at the same rate as the crossed polarizers. In the case of singularities with negative optical signs, the brushes rotate at the opposite rate as the crossed polarizers. The brushes are the regions where the director of liquid-crystalline structure is parallel or perpendicular to a polarization plane of the incident light. The singularities with the disclination of strength as both  $S = \pm \frac{1}{2}$  and  $S = \pm 1$  were found in this texture. Using Eqs. (3) and (4), the interaction forces per unit length between singularities with the disclination of strength as  $|S_1|=|S_2|=1$  and also as  $|S_1|=1$  and  $|S_2|=\frac{1}{2}$  were determined. These values were found for the first case as  $F_{12}=0.9 \times 10^{-6}-0.4 \times 10^{-6} \text{ N m}^{-1}$  and for the second case as  $F_{12}=0.5 \times 10^{-6}-0.3 \times 10^{-6} \text{ N m}^{-1}$ . It was also observed that the values of the interaction forces for  $N_C$  and  $N_D$  mesophases are approximately equal. This fact indicates that external magnetic field has similar deformational effect on  $N_C$  and  $N_D$  mesophases. After 6.5 h, a texture with large planar alignment regions was observed [Fig. 6(d)]. Finally, after 24.0 h under influence of magnetic field, texture presented in Fig. 6(e) has been observed. This texture consists of large separate regions with planar alignment. The birefringence of such separate regions was found to be  $\Delta n = 0.0047$ . As revealed by a comparison of the birefringence values for  $N_C$  and  $N_D$  mesophases of SLS-H<sub>2</sub>O-DeOH system, the above-mentioned values for  $N_D$  mesophase is somewhat greater than those for  $N_C$  mesophase. Such correlation between the birefringence values for mesophases was also observed in lyotropic systems based on sodium decylsulphate [75], tetradecyl trimethyl ammonium phenylsulphonate [76], and tetradecyldimethyl ammonium oxide [77,78]. Obviously, such situation is typical for  $N_C$  and  $N_D$  mesophases.

As seen in Fig. 6(g), separate regions with the planar alignment are divided by the sharp inversion walls. Optical investigations showed that these regions are characterized by the different displacements of the director, which are placed in the plane of the liquid-crystalline layer. Optical investigations also demonstrated that the inversion walls in this texture are placed perpendicularly to the liquid-crystalline layer. Thus, as revealed by a comparison of Figs. 5 and 6, the dynamics of the transformation of magnetically induced textures in  $N_D$  mesophase is somewhat different from such dynamics in  $N_C$  mesophase.

A comparison of the peculiarities of the magnetically induced textures and character of the aligned (planar) regions for both  $N_C$  and  $N_D$  mesophases indicates that in SLS-H<sub>2</sub>O-DeOH system  $N_C$  mesophase has  $\Delta\chi > 0$ , while  $N_D$  mesophase has  $\Delta\chi < 0$ . So in this lyotropic system  $N_C^+$  and  $N_D^-$  mesophases take place. We would like to note that in SDS-H<sub>2</sub>O-DeOH lyotropic system nematic-calamitic and nematic-discotic mesophases take place only as  $N_C^+$  and  $N_D^-$  mesophases [32]. Yet, for example, in lyotropic systems based on myristiltrimethyl ammonium bromide, myristiltrimethyl ammonium tholuolsulphate, and potassium laurate, nematic-calamitic and nematic-discotic mesophases take place as  $N_C^-$  and  $N_D^+$  mesophases [6,74,75]. Therefore, it can be concluded that possibly in ternary lyotropic systems based

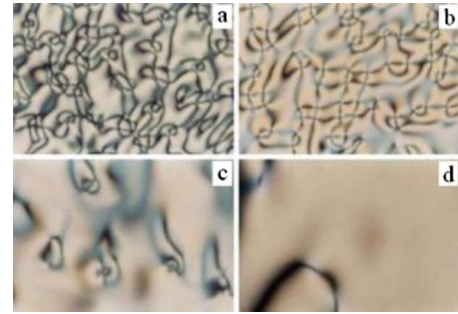


FIG. 7. (Color online) Magnetically induced textures of  $N_{bx}$  mesophase. Crossed polarizers. Magnification of  $\times 100$ . Temperature of 297.0 K. (a) After 1.5 h, (b) after 3.5 h, (c) after 6.0 h, and (d) after 24.0 h.

on sodium alkylsulphate,  $N_C$  mesophase has  $\Delta\chi > 0$  and  $N_D$  mesophase has  $\Delta\chi < 0$ .

$N_{bx}$  mesophase. Magnetic field has an essential effect on the morphologic properties of  $N_{bx}$  mesophase. Under the magnetic field, the texture presented in Fig. 7(a) was observed after 1.5 h. In this texture, the looplike formations take place, forming the boundaries between the planar alignment regions. The absence of the homeotropic regions in Fig. 7(a) indicates on the reorientation of axis with the magnetic susceptibility. After 3.5 h under the effect of magnetic field, the singular points and the wedge disclinations arose in the magnetically induced textures of  $N_{bx}$  mesophase [Fig. 7(b)]. As shown by optical investigations, in this texture optically positive and negative singular points take place with the disclination of strength as  $S = \pm \frac{1}{2}$  and  $S = \pm 1$ . Texture of such type has also been observed for  $N_{bx}$  mesophase in [79,80] for KL-D<sub>2</sub>O-DeOH lyotropic system. Then, the texture presented in Fig. 7(c) was observed after 6.0 h. As clear from a comparison of Figs. 7(c) and 7(d), magnetic field influence leads to a decrease in the density of the singular points and to an increase in planar oriented regions. It is also seen in Fig. 7(c) that in this texture, complicated inversion walls and singular points with the disclination of strength as  $S = \pm \frac{1}{2}$  and  $S = \pm 1$  are observed. After 24.0 h, the planar oriented texture with birefringence as  $\Delta n = 0.0047$  and rare singular points with the disclination of strength as  $S = \pm \frac{1}{2}$  were observed [Fig. 7(d)]. In this texture, the singular points with the integer disclination of strength as  $S = \pm 1$  are absent. This fact, in accordance with Eq. (2), is connected with the minimization of the energy of elastic distortions in  $N_{bx}$  mesophase under influence of external magnetic field. We would like to note that in the textures of  $N_C$  and  $N_D$  mesophases after 24.0 h under influence of magnetic field, the singular points were observed with the disclination of strength as  $S = \pm \frac{1}{2}$  and  $S = \pm 1$ . Because of such peculiarities of the magnetically induced textures,  $N_{bx}$  mesophase can be easily identified by the behavior of typical textures in magnetic field. We would also like to state that, as revealed by a comparison in Figs. 1(e) and 7, the effect of magnetic field leads to the disappearance of separate regions with the homeotropic alignment, indicating that magnetic field leads to a reorientation of the axis with magnetic susceptibility.

#### IV. CONCLUSION

In this work, the mesomorphic, thermomorphologic, thermotropic, and magnetomorphologic properties of SLS-water-DeOH lyotropic liquid-crystalline system have been investigated. This system displays the anisotropic E, D,  $N_C$ ,  $N_{bx}$ , and  $N_D$  mesophases. These mesophases are characterized by typical textures, taking place in strongly definite concentration and temperature intervals.

Investigations on the mesomorphic and thermotropic properties showed that the character of the triangle phase diagrams of SLS-water-DeOH lyotropic system, the concentration regions of lyotropic mesophases, and the number of these mesophases depend not only on the concentration ratio between system components but also on temperature.

Investigations on the dynamics of texture transformations demonstrated that external magnetic field affects the morphologic properties of E,  $N_C$ ,  $N_{bx}$ , and  $N_D$  mesophases. Magnetic field leads to an appearance of the loops, inversion walls, uniformly aligned regions, and also singularities with both positive and negative optical signs and the disclinations of strength as  $S = \pm 1$  and  $S = \pm \frac{1}{2}$ . On the other hand, external magnetic field did not have a sufficient effect on the morphologic properties of D mesophase.

Character of the aligned (planar) regions and peculiarities of the magnetically induced textures in  $N_C$  and  $N_D$  mesophases indicate that in SLS-H<sub>2</sub>O-DeOH system  $N_C$  mesophase has  $\Delta\chi > 0$  and  $N_D$  mesophase has  $\Delta\chi < 0$ .

Investigations revealed that the character of texture transformations in magnetic field and the morphologic properties of magnetically induced textures (density of loop formations,

character and displacement of the inversion walls, and character and the disclination of strength of the singular points) for  $N_C$ ,  $N_{bx}$ , and  $N_D$  mesophases are quite different. This fact gives a possibility to identify lyotropic nematic mesophases in lyotropic systems.

In this work the phase diagram of SLS-water-DeOH system for three different temperatures, typical stable textures, and magnetically induced textures of E, D,  $N_C$ ,  $N_{bx}$ , and  $N_D$  mesophases are presented. Interaction forces between various singularities in magnetically induced textures have been determined.

Finally, it is necessary to note that the rodlike and disklike micelles of lyotropic mesophases do not have a rigid structure and can change the shape, anisometricity, and form factor by a change of concentration and temperature [14,71,81]. Besides, the distances between micelles are not constant. They vary with varying temperature within interval of lyotropic mesophase [6,82]. Changes of orientational fluctuation may be taking place at the lyotropic and thermotropic phase transitions. These factors can lead to a change of phase boundaries between lyotropic liquid-crystalline mesophases and regions of above-mentioned mesophases.

#### ACKNOWLEDGMENTS

This work has been partially supported by the Research Foundation of Muğla University, Grants No. 2008/04. The authors are grateful to Dr. A. J. Palangana (Departamento de Física, Universidade Estadual Maringá) for textures of lyotropic nematic mesophases in potassium laurate–water–1-decanol system.

- 
- [1] P. Ekwall, *Adv. Liq. Cryst.* **1**, 1 (1975).
- [2] M. Angel, H. Hoffmann, M. Löbl, K. Reizlen, H. Thurn, and I. Wunderlich, *Prog. Colloid Polym. Sci.* **69**, 12 (1984).
- [3] A. G. Petrov, *Lyotropic State of Matter: Molecular Physics and Living Matter Physics* (Taylor & Francis, London, England, 1999).
- [4] A. M. Figueiredo Neto and S. R. A. Salinas, *The Physics of Lyotropic Liquid Crystals: Phase Transitions and Structural Properties* (Oxford University Press, Oxford, 2005).
- [5] A. Nesrullajev, *Lyotropic Liquid Crystals: Amphiphilic Systems* (Mugla University Press, Mugla, 2007).
- [6] A. S. Sonin, *Sov. Phys. Usp.* **30**, 875 (1987).
- [7] G. Hertel, Ph.D. dissertation, Bayreuth University, 1989.
- [8] A. A. de Melo Filho, N. S. Amadeu, and F. Y. Fujiwara, *Liq. Cryst.* **34**, 638 (2007).
- [9] M. R. Kuzma, *Phys. Rev. Lett.* **57**, 349 (1986).
- [10] U. Kaeder and K. Hiltrop, *Prog. Colloid Polym. Sci.* **84**, 250 (1991).
- [11] P. A. Santoro, A. R. Sampaio, H. L. F. da Luz, and A. J. Palangana, *Phys. Lett. A* **353**, 512 (2006).
- [12] C. Quilliet, V. Ponsinet, and V. Cabuil, *J. Phys. Chem.* **98**, 3566 (1994).
- [13] A. Nesrullajev and Ş. Oktik, *Cryst. Res. Technol.* **42**, 44 (2007).
- [14] A. Nesrullajev, D.Sc. dissertation, National Academy of Sciences, 1992.
- [15] A. Nesrullajev, S. Salihoglu, and H. Yurtseven, *Int. J. Mod. Phys. B* **12**, 213 (1998).
- [16] S. Yıldız and A. Nesrullajev, *Physica A* **385**, 25 (2007).
- [17] J. Nehring and A. Saupe, *J. Chem. Soc., Faraday Trans. 1* **68**, 1 (1972).
- [18] J. E. Zimmer, Ph.D. thesis, Purdue University, 1978.
- [19] J. L. White and J. E. Zimmer, *Carbon* **16**, 469 (1978).
- [20] J. E. Zimmer and J. L. White, *Adv. Liq. Cryst.* **5**, 159 (1982).
- [21] J. Lydon, in *Handbook of Liquid Crystals*, edited by D. Demus, J. Goodby, G. W. Gray, H.-W. Spiess, and V. Vill (Wiley-VCH, Weinheim, 1998), Vol. IIB, p. 981.
- [22] A. Nesrullajev, M. Tepe, D. Abukay, N. Kazancı, D. Demirhan, and F. Büyükkılıç, *Appl. Phys. A: Mater. Sci. Process.* **71**, 161 (2000).
- [23] I. D. Leigh, M. P. McDonald, R. M. Wood, G. J. T. Tiddy, and M. A. Trevelyan, *J. Chem. Soc., Faraday Trans. 1* **77**, 2867 (1981).
- [24] H. Sagatami and S. E. Friberg, *Bull. Chem. Soc. Jpn.* **56**, 31 (1983).
- [25] A. Nesrullajev, F. Rustamov, and A. Sonin, *Crystallography* **29**, 1133 (1984).
- [26] A. M. F. Neto, A. M. Galerne, Y. Levelut, and L. Liebert, J.

- Phys. (France) Lett. **46**, 499 (1985).
- [27] L. Q. Amaral, M. E. Helene, D. R. Bittencourt, and R. Itri, *J. Phys. Chem.* **91**, 5949 (1987).
- [28] L. Q. Amaral and M. E. Marcondes Helene, *J. Phys. Chem.* **92**, 6094 (1988).
- [29] P. Kekicheff, O. Gabrielle Madelmont, and M. Ollivon, *J. Colloid Interface Sci.* **131**, 112 (1989).
- [30] P. Quist, B. Halle, and I. Furo, *J. Phys. Chem.* **96**, 3875 (1992).
- [31] I. Furo and B. Halle, *Phys. Rev. E* **51**, 466 (1995).
- [32] P.-O. Quist, *Liq. Cryst.* **18**, 623 (1995).
- [33] O. Santin Fulho, R. Itri, and L. Q. Amaral, *J. Phys. Chem. B* **104**, 959 (2000).
- [34] L. Q. Amaral, *Braz. J. Phys.* **32**, 540 (2002).
- [35] [http://wapedia.mobi/en/Hexagonal\\_phase](http://wapedia.mobi/en/Hexagonal_phase)
- [36] A. Nesrullajev, M. Tepe, N. Kazanci, H. M. Çakmak, and D. Abukay, *Mater. Chem. Phys.* **65**, 125 (2000).
- [37] A. Nesrullajev, M. Okcan, and N. Kazanci, *J. Mol. Liq.* **108**, 313 (2003).
- [38] H. D. Dörfler and A. Göpfert, *Colloid Polym. Sci.* **278**, 1085 (2000).
- [39] H. D. Dörfler, *Adv. Colloid Interface Sci.* **98**, 285 (2002).
- [40] S. Ujiie and Y. Yano, *Chem. Commun. (Cambridge)* **2000**, 79.
- [41] A. Saupe, *J. Colloid Interface Sci.* **58**, 549 (1977).
- [42] I. G. Chistyakov, *Liquid Crystals* (Science Publication, Moscow, 1966).
- [43] V. A. Belyakov and A. S. Sonin, *Optics of Cholesteric Liquid Crystals* (Science Publication, Moscow, 1982).
- [44] <http://bly.colorado.edu/lcphysics/textures/>
- [45] I. Dierking, *Textures of Liquid Crystals* (Wiley-VCH, Weinheim, 2003).
- [46] I. Dierking, F. Giesselmann, P. Zugenmaier, W. Kuczynski, S. T. Lagerwall, and B. Stebler, *Liq. Cryst.* **13**, 45 (1993).
- [47] G. Hertel and H. Hoffmann, *Prog. Colloid Polym. Sci.* **76**, 123 (1989).
- [48] H. Hoffmann, G. Oetter, and B. Schwandner, *Prog. Colloid Polym. Sci.* **73**, 95 (1987).
- [49] M. R. Kuzma and A. Saupe, in *Handbook of Liquid Crystal Research*, edited by P. J. Collings and J. S. Patel (Oxford University Press, New York, 1997), p. 237.
- [50] A. R. Sampaio, A. J. Palangana, and R. C. Visconini, *Mol. Cryst. Liq. Cryst.* **408**, 45 (2004).
- [51] A. J. Palangana (private communication).
- [52] G. Bartusch, H.-G. Dörfler, and H. Hoffmann, *Prog. Colloid Polym. Sci.* **89**, 307 (1992).
- [53] E. Govers and G. Vertogen, *Phys. Rev. A* **30**, 1998 (1984).
- [54] G. Burducea, *Rom. Rep. Phys.* **56**, 66 (2004).
- [55] R. Bartolino, T. Chiaranza, M. Meuti, and R. Compagnoni, *Phys. Rev. A* **26**, 1116 (1982).
- [56] R. Bartolino, M. Meuti, G. Chidichimo, and G. A. Ranieri, in *Physics of Amphiphiles: Micelles, Vesicles and Microemulsions*, edited by V. Degiorgio and M. Corti (North Holland Press, Amsterdam, 1985), p. 524.
- [57] L. J. Yu and A. Saupe, *Phys. Rev. Lett.* **45**, 1000 (1980).
- [58] Y. Galerne and J. P. Marcerou, *Phys. Rev. Lett.* **51**, 2109 (1983).
- [59] S. Emid, J. Konijnendijk, J. Smidt, and A. Pines, *Physica B & C* **100**, 215 (1980).
- [60] A. Saupe, *Nuovo Cimento* **3**, 16 (1984).
- [61] I. Furo and B. Halle, *J. Chem. Phys.* **91**, 42 (1989).
- [62] M. J. Freiser, *Phys. Rev. Lett.* **24**, 1041 (1970).
- [63] I. Furo, B. Halle, and L. Einarsson, *Chem. Phys. Lett.* **182**, 547 (1991).
- [64] P.-O. Quist, B. Halle, and I. Furo, *J. Chem. Phys.* **95**, 6945 (1991).
- [65] S. M. Gudilov, E. L. Kitaeva, and A. S. Sonin, *Crystallography* **31**, 537 (1986).
- [66] M. Simoes, A. J. Palangana, and L. R. Evangelista, *Phys. Rev. E* **54**, 3765 (1996).
- [67] A. S. Sonin, *Introduction to the Physics of Liquid Crystals* (Science Publication, Moscow, 1983).
- [68] S. Chandrasekhar, *Liquid Crystals* (Cambridge University, Cambridge, 1992).
- [69] P. G. de Gennes and J. Prost, *The Physics of Liquid Crystals* (Oxford Science Publication, Oxford, 1993).
- [70] E. V. Generalova, A. V. Kaznacheev, and A. S. Sonin, *Crystallogr. Rep.* **46**, 111 (2001).
- [71] A. R. Sampaio, N. M. Kimura, R. C. Viscovini, P. R. G. Fernandes, and A. J. Palangana, *Mol. Cryst. Liq. Cryst.* **422**, 57 (2004).
- [72] E. Guyen, R. Meyer, and J. Salan, *Mol. Cryst. Liq. Cryst.* **54**, 261 (1979).
- [73] S. Chandrasekhar, *Liquid Crystals* (Cambridge University, Cambridge, 1977).
- [74] M. C. Holmes, N. Boden, and K. Radley, *Mol. Cryst. Liq. Cryst.* **100**, 93 (1983).
- [75] M. Meuti, G. Barbero, R. Bartolino, T. Chiaranza, and E. Simoni, *Nuovo Cimento* **3**, 30 (1984).
- [76] K. Radley, *Mol. Cryst. Liq. Cryst. Lett.* **102**, 113 (1984).
- [77] A. Nesrullajev and N. Kazanci, *Mater. Chem. Phys.* **62**, 230 (2000).
- [78] N. Kazanci and A. Nesrullajev, *Mater. Res. Bull.* **38**, 1003 (2003).
- [79] D. A. Oliveira, D. D. Luders, G. P. Souza, N. M. Kimura, and A. J. Palangana, *Cryst. Res. Technol.* **44**, 1255 (2009).
- [80] M. Simoes, A. J. Palangana, L. R. Evangelista, W. S. Braga, and F. S. Alves, *Phys. Rev. E* **72**, 031707 (2005).
- [81] A. Nesrullajev, *Mater. Chem. Phys.* **123**, 546 (2010).
- [82] Y. Galerne, A. M. Figueiredo Neto, and L. Liebert, *Phys. Rev. A* **31**, 4047 (1985).